Cellular and Molecular Bioengineering, Vol. 9, No. 1, March 2016 (© 2015) pp. 107–115
DOI: 10.1007/s12195-015-0412-9

Biomimetic Microstructure Morphology in Electrospun Fiber Mats is Critical for Maintaining Healthy Cardiomyocyte Phenotype

RUTWIK RATH,[1] JUNG BOK LEE,[1] TRUC-LINH TRAN,[2] SEAN F. LENIHAN,[2] CRISTI L. GALINDO,[2] YAN RU SU,[2] TAREK ABSI,[3] LEON M. BELLAN,[1,4] DOUGLAS B. SAWYER,[2] and HAK-JOON SUNG[1,2]

[1]Department of Biomedical Engineering, Vanderbilt University, Nashville, TN, USA; [2]Cardiovascular Division, Department of Medicine, Vanderbilt University, Nashville, TN, USA; [3]Department of Cardiothoracic Surgery, Vanderbilt University, Nashville, TN, USA; and [4]Department of Mechanical Engineering, Vanderbilt University, Nashville, TN, USA

(*Received 9 April 2015; accepted 20 July 2015; published online 8 September 2015*)

Associate Editor Tanmay Lele oversaw the review of this article.

Abstract—Despite recent advances in biomimetic substrates, there is still only limited understanding of how the extracellular matrix (ECM) functions in the maintenance of cardiomyocyte (CM) phenotype. In this study, we designed electrospun substrates inspired by morphologic features of non-failing and failing human heart ECM, and examined how these substrates regulate phenotypes of adult and neonatal rat ventricular CMs (ARVM and NRVM, respectively). We found that poly(ε-caprolactone) fiber substrates designed to mimic the organized ECM of a non-failing human heart maintained healthy CM phenotype (evidenced by cell morphology, organized actin/myomesin bands and expression of β-MYH7 and SCN5A.1 and SCN5A.2) compared to both failing heart ECM-mimetic substrates and tissue culture plates. Moreover, culture of ARVMs and NRVMs on aligned substrates showed differences in *m*- and *z*-line alignment; with ARVMs aligning parallel to the ECM fibers and the NRVMs aligning perpendicular to the fibers. The results provide new insight into cardiac tissue engineering by illustrating the importance models that mimic the cardiac ECM microenvironment *in vitro*.

Keywords—Electrospinning, Poly(ε-caprolactone), Cell–matrix interaction, Cardiomyocyte, Cell phenotype.

INTRODUCTION

Although various cardiomyocyte (CM) culture environments have been investigated, one that maintains a healthy, physiologically relevant adult CM phenotype has yet to be fully developed.[36] One of the most widely used clinical CM models involves the use of rodent neonatal ventricular CMs (NRVMs) on tissue culture plates (TCPS). This model is popular because of its versatility[38] and convenience, compared to whole animal heart experiments.[7] Research with this model has enabled morphological, biochemical and electrophysiological characterization of the heart,[29] providing insight into the contraction, ischemia, hypoxia and toxicity of various compounds.[7] These studies, however, are severely limited by the phenotypic changes CMs undergo when cultured *in vitro*;[5] with the cells demonstrating altered gene expression (such as induction of smooth muscle α-actin)[34] and changes in morphology[15] compared to CMs *in vivo*.[2]

Significant progress has been made in developing culture models mimicking the cardiac environment. As a result, important CM matrix parameters have been successfully studied including: matrix fiber alignment,[45] mechanical strain,[19] matrix stiffness,[3] nanoscale mechanical cues[23] and three dimensional structure (such as accordion-like honeycombs[11,12]). However, none of these models have been used to elucidate how healthy and diseased cardiac extracellular matrix (ECM) environments manifest in variations of matrix fiber spacing, diameter, and alignment at the micro-scale. Even though it is hypothesized that these parameters regulate CM behavior *in vitro*, identifying the characteristics of cardiac ECM that are critical for retaining the *in vivo* CM phenotype is a necessary first step to fully understand the complex cell-ECM interplay *in vitro*. Thus, although ECM composition, stiffness, and organization[4,26] have been considered important regulators of CM phenotype,[40] precise understanding of how ECM structure maintains CM phenotype needs to be further elucidated.[35,40]

In this study, we investigated how key morphological ECM parameters from non-failing and failing human hearts (fiber alignment, spacing, and diameter)

Address correspondence to Douglas B. Sawyer and Hak-Joon Sung, Cardiovascular Division, Department of Medicine, Vanderbilt University, Nashville, TN, USA. Electronic mails: douglas.b.sawyer@vanderbilt.edu and hak-joon.sung@vanderbilt.edu

regulate CM morphology, actin/myomesin patterning, and cardiac gene expression. We found that aligned poly(ε-caprolactone) (PCL) substrates enhanced the preservation of adult rat ventricular CM (ARVM) phenotype *in vitro* as evidenced by longer/more rod shaped morphology, sarcomere organization, and gene expression. These findings provide insights into ECM-CM interactions that are responsible for maintenance/loss of ARVM and NRVM phenotypes, and highlight the importance of developing relevant culture substrates for *in vitro* studies.

MATERIALS AND METHODS

Human Tissue Procurement and Scanning Electron Microscopy

Left ventricular tissue was collected from human subjects under a protocol approved by the Vanderbilt Institutional Review Board. Non-failing human myocardium was collected from human donors with tissue unable to be used for heart transplant. Failing human donor specimens were collected from explanted hearts at the time of heart transplant. Specimens were taken directly at the time of collection in the operating room and fixed in 4% glutaraldehyde in a 0.1 M phosphate buffer solution and stored at 4 °C. Tissues were macerated in 10% aqueous NaOH for 10 days to maintain fibrous structure of cardiac tissue ECM while removing non-fibrous elements. Fixation, critical point drying, and sputter coating were performed in the Vanderbilt Cell Imaging Shared Resource Core. Images were acquired using the FEI Quanta 250 field emission gun scanning electron microscope (SEM), which was operated in high vacuum mode, at an accelerating voltage of 8 or 10 kV.

Electrospun PCL Substrates and SEM Imaging

Fiber substrates were fabricated by electrospinning a 12.5 wt.% solution of PCL (Sigma-Aldrich, 80 kDa) dissolved in a 4:1 volume solution of chloroform (Sigma-Aldrich): methanol (Sigma-Aldrich). The solution was mixed *via* continuous vortexing, and loaded into a 3 cc plastic syringe (Cadence Science) fitted with a 22-gage blunt tip stainless steel needle (EFD Precision Tips). Fibers were electrospun using an electrospinner (NABOND Nano E-spinning System) set between 9 and 10 kV at a 10 cm collection distance with a 0.2–0.5 mL/h flow rate. PCL fibers were deposited for 5 min onto either parallel wire-collectors with a spacing of 1.5 cm (aligned fibers) or a slowly rotating drum (less aligned fibers) setup onto 15 mm rubber O-rings (McMaster-Carr), creating a suspended fiber format so CMs could only adhere onto the fiber substrates (Supplementary Figs. 1, 2). The O-rings supporting PCL fibers were placed overnight in a vacuum to remove residual solvents. The dried fibers were then placed between 1 mm thick PDMS O-rings with an outer diameter of 12 mm and an inner diameter of 8 mm (Miltex® Biopsy Punch) to maintain the organized structure of the fibers while preserving the elasticity of the PCL. PCL fiber substrates were immersed in ethanol to remove residual solvent followed by drying in vacuum overnight prior to other experiences. For the SEM imaging, dried samples were sputter coated with an ATC 2200 gold sputter coater (AJA International, Inc.) for 60 s and imaged by SEM (Hitachi S4200).

PCL control substrates were fabricated by spin-coating with 1 wt.% PCL solution dissolved in THF (Sigma-Aldrich). 50 μL of solution was placed onto a clean 15 mm glass coverslip that was loaded into a spin coater (WS-650SZ-6WPP/LITE Spin Coater, Laurell Technologies). The coverslip was accelerated to 3000 rpm at 500 rpm/s for 30 s at RT. Once complete, the coverslips were removed and dried overnight under vacuum prior to sterilization and use as material control substrates.

CM Isolation and Culture on Substrates

All animal procedures were conducted according to the guidelines of the Vanderbilt University Animal Care and Use Committee under an approved protocol. Ventricular CMs from 2-day old and 7 week old rat hearts, for NRVMs and ARVMs respectively, were isolated and cultured using previously described protocols.[4,11] PCL substrates were sterilized for 1 h under UV and incubated with 250 μL of 10 mg/mL whole mouse laminin (Fisher) for 2 h at room temperature for surface coating. CMs were then seeded at 60,000 cells/cm^2 and allowed to adhere for 3 h in DMEM(-Sigma) + 7% bovine serum (Sigma) containing 0.1 mM BrdU to prevent division and over growth of non-CM cells (Sigma) and 25 μM blebbistatin to prevent hypercontraction-mediated death[21] CMs were then switched to defined serum-free media consisting of DMEM (Gibco), 2 mmol/L L-glutamine, 2 mmol/L pyruvate, 25 mmol/L HEPES, and pH 7.4 $NaHCO_3$ (Sigma) supplemented with 2 mg/mL BSA, 2 mmol/L L-carnitine, 5 mmol/L creatine, and 5 mmol/L taurine, with 100 IU/mL penicillin and 100 μg/mL streptomycin (Gibco), as described previously for phenotypic studies[10] and cultured overnight (12–15 h) with 25 μM blebbistatin. The next day, CMs were incubated for 1 h in serum free media + 20 mM KCl (Sigma) (without blebbistatin) to allow for the reforming of sarcomere structures in diastole.[39] These CMs were

then fixed or treated for the appropriate endpoint assays.

CM Morphology, Alignment, and Fiber Parameter Analysis

CMs were cultured and analyzed for morphology and alignment in substrates placed in a 24 well plate. For high resolution imaging of cells, the substrates were moved from the O-ring setup in a 24 well plate onto a cover glass after fixing and staining processes were done. For all CMs, CMs were fixed in 4% paraformaldehyde solution and imaged on a Nikon Eclipse Ti inverted fluorescence microscope. The images were then imported into ImageJ (NIH, Bethesda, MA) and analyzed for CM morphology (i.e., aspect ratio), CM/sarcomere/fiber alignment, and substrate spacing and diameter using the methods reported previously.[44] For cell aspect ratio, the first line was drawn along the longest length of each cell, followed by drawing a second line perpendicular to the first line. The aspect ratio was determined by taking the longest length and dividing it by the length of the perpendicular line. A total of 25 measurements made on three different SEM images (containing at least 5 fibers/cells), each representing a non-overlapping random field of view for each type of CM culture substrate, was analyzed.

Immunofluorescence Staining

CMs were permeabilized overnight in 0.2% Triton X-100 at 4 °C and then blocked overnight with PBS containing 20% goat serum and 0.2% Triton X-100 at 4 °C. CMs were then incubated overnight with a solution of 1:200 primary mouse anti-myomesin antibody (C-16, Santa Cruz Biotechnology) diluted in PBS containing 0.1% BSA and 0.2% Triton X-100 (antibody solution) at 4 °C on a shaker at low speed, followed by overnight incubation in a solution of 1:200 secondary goat anti-mouse Alexa 594-conjugated antibody (Abcam) at 4 °C in the dark on a shaker at low speed. After 18 h, the CMs were rinsed and incubated in 200 μL of 0.0016 μM Hoechst dye for 10 min at room temperature and then incubated for 20 min in 200 μL of 0.16 μM AlexaFluor 488-conjugated Phalloidin (Life Tech, Carlsbad, CA) at RT. CMs were imaged on the Nikon Eclipse Ti inverted fluorescence microscope, and the average widths of the actin and myomesin bands were analyzed in ImageJ (NIH, Bethesda, MA).

Conventional Polymerase Chain Reaction (PCR)

For PCR, 15 ng cDNA was prepared by Trizol (Life-Tech) isolation, followed by synthesis (Life-Tech) of cDNA using the manufacture's recommended protocol. The cDNA was mixed with PCR Master Mix (Life Tech) and 500 nM mRNA-specific primers for the specified genes. Samples were then amplified in a PCR machine (Bio-Rad, model S1000) with the following steps: 3 min at 95 °C to denature DNA, followed by 35 steps of 95 °C for 30 s (denaturation), 58 °C for 30 s (annealing), and 72 °C for 30 s (extension). Genes of interest included myosin heavy chain 6 and 7, sodium-voltage gated channel 5 isoform 1 and 2, and α-smooth muscle actin (Table 1). Expression was normalized to 60 s ribosomal protein L4 (RPL4).

Statistical Analysis

Data is presented as mean ± standard error mean for all except fiber alignment. Average and standard deviations were calculated in Excel (Microsoft, Redmond, WA) and imported into GraphPad Prism (GraphPad Software, La Jolla, CA). Data was analyzed using a one-way ANOVA and if significance was found, tested using a Bonferroni *post hoc* test ($p < 0.05$ was considered significant).

RESULTS

Engineering Substrates to Mimic Non-failing and Failing ECM

ECM fiber structures were examined in decellularized human heart tissues (Fig. 1). The ECM of a non-failing human heart shows an aligned fibril organization that wraps around individual CMs (Fig. 1a). The aligned fibers are perpendicular to the long axis of the

TABLE 1. Sequences of primers used in conventional polymerase chain reaction (cPCR).

Primer name	Forward primer sequence	Reverse primer sequence
α-MYH6	AGGAGGCACTGATTTGGCAG	GGGAGGTCTGTAGGGAGTCCA
β-MYH7	CGAGAGATGGCTGCATTTGG	TGGACTGGTTCTCCCGATCT
SCN5A.1	GTGGATCGAGACCATGTGGG	GCCGTCTGCCTGAGATGTA
SCN5A.2	CTGTGCTACGTTCCTTCCGT	ACGTCCTCAGGGGTCTGTT
α-SMA	CAGTCGCCATSAGGAACCTC	CTGTCAGCAATGCCTGGGTA
RPL4	GAGTTGTATGGCACTTGGCG	TGCGTAAGGGTTCAGCTTCA

Forward and reverse primers are shown.

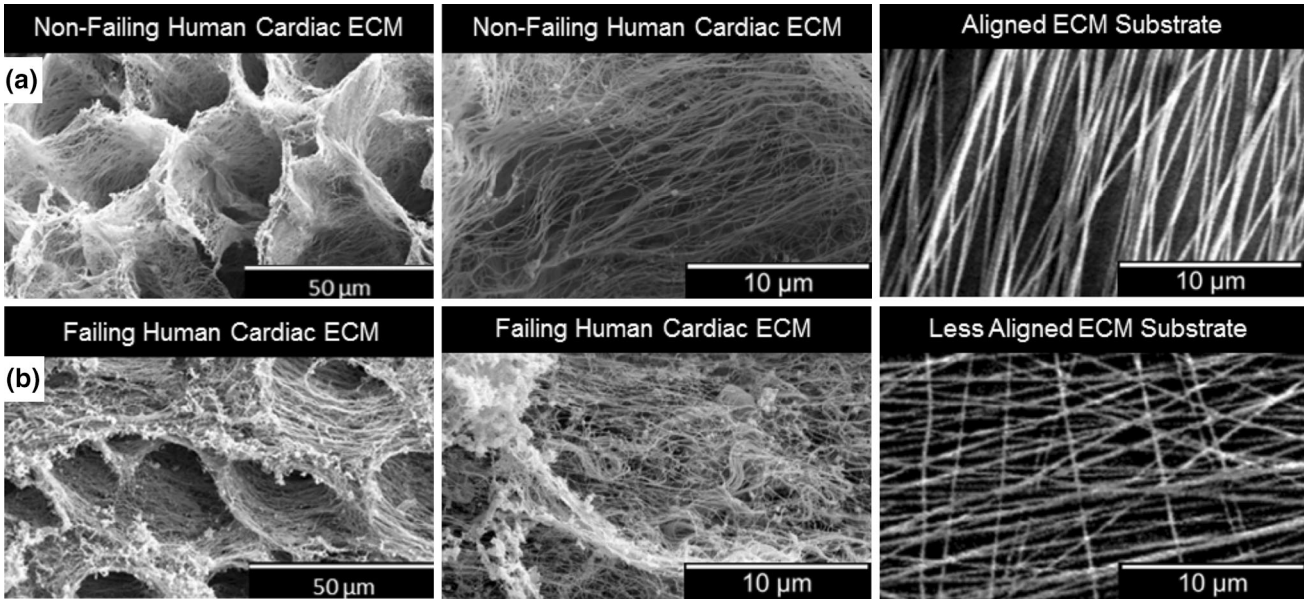

FIGURE 1. Characterization of decellularized human cardiac ECM and PCL fiber substrates. Representative scanning electron microscopy (SEM) images of (a) non-failing human cardiac ECM and aligned fiber substrate and (b) failing human cardiac ECM and less aligned fiber substrate.

TABLE 2. Analysis of alignment variation, fiber spacing, and fiber diameter of non-failing/failing human cardiac ECM and aligned/less aligned ECM substrates.

Test groups	Alignment variation (°)	Fiber spacing (μm)	Fiber diameter (μm)
Non-failing human cardiac ECM	-8 ± 2:$+2 \pm 3$	0.15 ± 0.04	0.47 ± 0.52
Aligned ECM substrate	-6 ± 1:$+2 \pm 3$	0.12 ± 0.07	0.42 ± 0.37
Failing human cardiac ECM	-15 ± 45:$+20 \pm 30$	0.35 ± 0.19	0.15 ± 0.14
Less aligned ECM substrate	-30 ± 25:$+15 \pm 30$	0.43 ± 0.24	0.23 ± 0.11

CMs and aligned with the cardiac sarcomeres, thereby enhancing the compressibility of the ECM during sarcomere shortening.[20,33] In contrast, the alignment of the ECM in a failing human heart is significantly diminished (Fig. 1b). These results are supported by our previous work using a large animal model.[14]

To mimic these ECM fiber structures, electrospinning parameters were optimized to generate aligned and less aligned fiber substrates, which were compared to those of natural ECM in terms of fiber alignment, spacing, and diameter (Table 2). Non-failing ECM and aligned fiber substrates were similarly aligned (-8 ± 2:$+2 \pm 3°$ and -6 ± 1:$+2 \pm 3°$ respectively), as were the failing ECM and less aligned fiber substrates (-15 ± 45:$+20 \pm 30°$ and -30 ± 25:$+15 \pm 30°$ respectively). Non-failing ECM fiber spacing ($N = 14$, 0.15 ± 0.04 μm) and diameter ($N = 13$, 0.47 ± 0.52 μm) were similar to aligned fiber substrate spacing ($N = 25$, 0.12 ± 0.07 μm) and diameter ($N = 35$, 0.42 ± 0.37 μm). Failing ECM fiber spacing ($N = 30$, 0.35 ± 0.19 μm) and diameter ($N = 7$, 0.15 ± 0.14 μm) were similar to less aligned fiber substrate spacing ($N = 25$, 0.43 ± 0.24 μm) and diameter ($N = 8$, 0.23 ± 0.11 μm). Thus we were able to create electrospun fiber substrates with similar fiber alignment, spacing and diameter to the non-failing and failing human heart.

Actin/Myomesin Staining of ARVM and NVRVMs and Quantification of ARVM/ARVM Sarcomere Alignment on Aligned fibers

To determine the influence of substrate fiber organization on phenotype changes in CMs, ARVMs and NRVMs were cultured on the test substrates and immunofluorescently stained (IF staining) for actin and myomesin (component of myosin) (Figs. 2a–2d). Additional images can be found in Supplementary Fig. 3. NRVMs cultured on aligned fibers adhered and elongated in the parallel direction of substrate fiber alignment, with sarcomeres organized perpendicular to alignment, while NRVMs on less aligned substrates showed unorganized sarcomere structures. On the

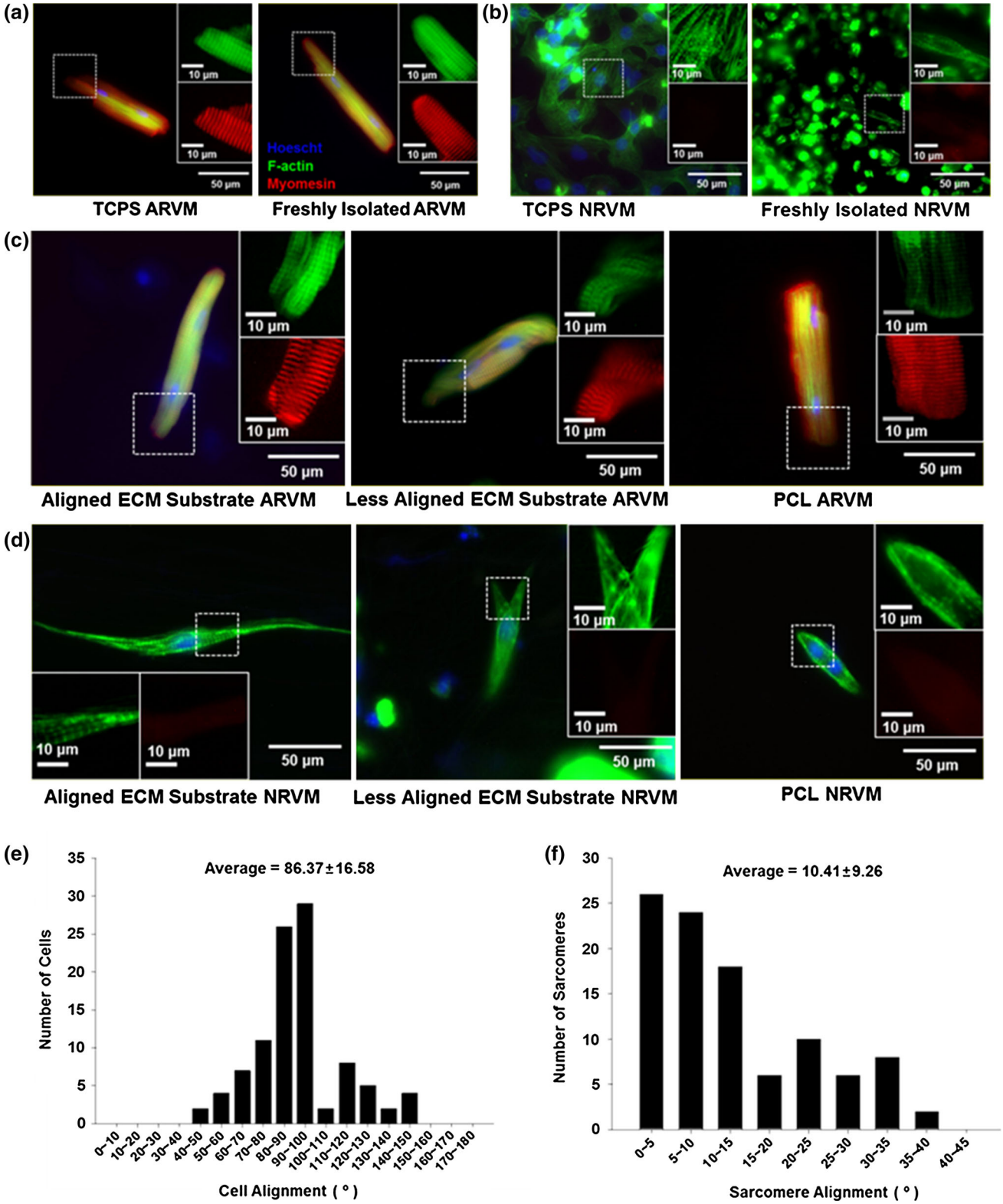

FIGURE 2. Actin/myomesin staining of adult and neonatal CMs and quantification of ARVM/ARVM sarcomere alignment on aligned fibers. Actin/myomesin band staining of freshly isolated and tissue culture polystyrene (TCPS)-cultured (a) ARVMs and (b) NRVMs. The same staining for aligned fiber substrate-cultured, less aligned fiber substrate-cultured, and spin-coated polymer control (PCL)-cultured of (c) ARVMs and (d) NRVMs. White squares correspond to the enlarged images and indicate channels of actin (green) and myomesin (red). Degree of ARVM cell (e) and corresponding sarcomere (f) alignment vs. aligned fibers.

other hand, ARVMs adhered to the substrates with the long-axis perpendicular to the aligned fibers (Fig. 2e, $N = 100$, $86.37° \pm 16.58°$). IF staining showed preserved sarcomere structure in ARVMs cultured on aligned substrates, with m- and z-lines parallel to the aligned fibers (Fig. 2f, $N = 100$, $10.41° \pm 9.26°$). While the sarcomere structure of ARVMs cultured on less aligned fiber substrates was not well-preserved.

Morphological and Cardiac Gene Expression of ARVMs

To determine whether aligned fiber substrates altered ARVM phenotype, ARVMs were cultured and imaged by SEM (Fig. 3a). Additional images can be found in Supplementary Fig. 4. Analysis of the CM morphology indicates that ARVMs cultured on aligned fiber substrates preserved their length/width ratios when compared to those on less aligned fiber and spin-coated substrates (Fig. 3b). While NRVMs followed a similar trend, with NRVMs cultured on aligned fiber substrates having significantly higher aspect ratios (Fig. 3c), the NRVMs grew parallel to the aligned fibers (as noted above). ARVMs cultured on aligned fiber substrates maintained a highly polar cylindrical morphology while ARVMs cultured on less aligned fiber substrates and spin-coated substrates appeared shortened and disorganized.

These phenotypic changes of ARVMs were further investigated by PCR (Fig. 3d). The expression of cardiac sarcomere *β-MYH7* and voltage gated sodium ion channels (SCN5A) was visibly lower in ARVMs on TCPS compared to those in the freshly isolated and both fiber substrate–cultured ARVMs. Thus, the electrospun fiber substrates appear to enhance preservation of sarcomere gene expression in ARVMs. Unexpectedly, reduced expression of *α-MYH6* was seen under all the conditions compared to freshly isolated ARVMs.

Analysis from our data indicated the CM morphology changed on TCPS and spin-coated substrate. There was a substantial effect of fiber alignment on preservation of CM morphology. Overall, this study supports the concept that ECM structure controls CM phenotype by promoting or preventing ultrastructure re-organization in CMs.

DISCUSSION

Most *in vitro* experimental work with CMs use TCPS. Culture on TCPS allows for the direct manipulation of CMs without interference from compensatory feedback mechanisms *in vivo*.[6] CMs cultured on TCPS, however, typically remain rod-shaped and cross-striated for 24–48 h before becoming more rounded at the ends, and ultimately re-organizing their sarcomeres.[5] Various methods have been used to minimize rounding and sarcomere reorganization, including blebbistatin (a specific and reversible myosin II inhibitor)[22,25] and plating decellularized ECM.[8,30,41] However, there is still significant work needed to create

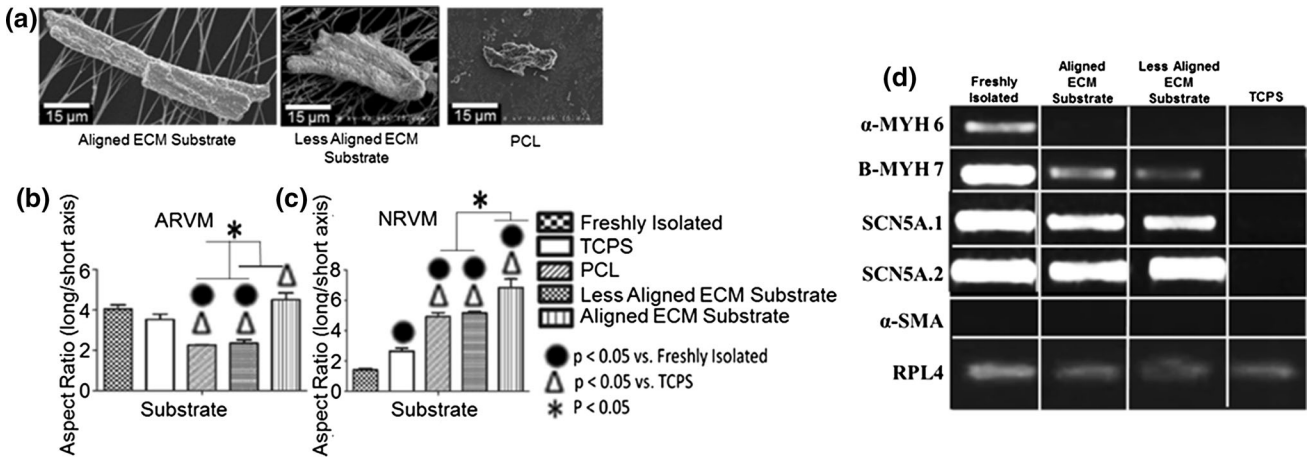

FIGURE 3. SEM imaging, morphology analysis, and cPCR analysis of adult CMs. (a) SEM images of adult CMs on aligned ECM substrate (left), less aligned ECM substrate (middle) and spin-coated substrate (right). Morphology analysis of CM aspect ratio of (b) ARVMs and (c) NRVMs cultured on various substrates. ARVMs cultured on aligned fiber substrates have greater aspect ratios vs. all other ARVM groups except for TCPS-cultured and freshly isolated ARVMs while NRVMs on aligned fiber substrates have the greatest aspect ratio vs. all the other NRVM groups.*$p < 0.05$. (d) PCR analysis of adult CMs indicates continued expression of β-MYH7 and SCN5A1 and SCN5A2 (without activation of α-smooth muscle actin) on cells cultured on electrospun fiber substrates, with complete suppression of all genes on TCPS. α-MYH6—Alpha Myosin Heavy Chain 6; β-MYH7—Beta Myosin Heavy Chain 7; 5A 1—Sodium Channel, voltage-gated type 5 isoform 1; SCN5A 2—Sodium Channel, voltage-gated type 5 isoform 2; α-SMA—Alpha Smooth Muscle Actin; RPL4—60S ribosomal protein L4 (housekeeping control).

substrates that better mimic the organization of cardiac ECM.

Hence, we created synthetic substrates using a widely used polymer (PCL)[9] with a modulus similar to cardiac tissue[28,42] (reported in our previous study[16]). This polymer was spin-coated into a flat uniform sheet (as a control with morphology similar to TCPS) as well as electrospun into aligned/less aligned fibers to create structures similar to those found in the human heart.[37] Our data (Fig. 3) indicated that, though there was a change in CM morphology between TCPS and control PCL, aligned fiber substrates were best at maintaining the CM striation pattern and reducing rounding. A substrate of the same composition but less aligned organization resulted in an accelerated rounding and loss of striation pattern, supporting the idea that ECM structure controls CM phenotype by promoting or preventing ultrastructure re-organization in CMs.

In healthy human ventricles, diastolic CM aspect ratio (AR) is tightly regulated to be approximately 7:1 length/width.[27] AR is critical in determining the contractile performance,[36] with its shape affecting calcium metabolism.[24,37] We observed that fiber alignment and the resulting controlled spacing between fibers regulated CM AR (Fig. 3b) and cell alignment (Figs. 2e–2f) by providing anchor points (Supplementary Fig. 2). CMs can adhere and adapt to these anchor points, thereby maintain their phenotypes.

These changes were further reflected at the gene level. In healthy adult CMs, alpha-myosin heavy chain (alpha-MHC, also known as Myh6) is expressed more dominantly than beta-MHC (also known as Myh7).[17,18] Cardiac stress triggers adult hearts to undergo hypertrophy and a shift from alpha-MHC to beta-MHC expression. CMs expressing beta-MHC, however, are still able to produce maximal isometric force but with altered force–velocity relationships and decreased loaded shortening velocities and power generation.[18] The expression of sodium channels (SCN5A) with the lack of specifically re-expressed of smooth muscle α-actin fetal gene[34] in the CMs on fiber substrates suggests that adult phenotype of CMs cultured on fibers was not irreversibly changed but partially altered. CMs cultured on TCPS, on the other hand, lacked expression of both myosin heavy chains and sodium voltage gated channels, suggesting that these CMs genetically and phenotypically lost functional contractile phenotypes.[32]

Finally, and most interestingly, a change in level of alignment also resulted in a difference in relative orientation of cells and sarcomeres (with respect to aligned fibers) for ARVMs and NRVMs. The m- and z-lines were parallel to the aligned fibers in ARVMs but perpendicular to the aligned fibers in NRVMs. This difference is likely due to the state of sarcomere and, more generally, cytoskeleton organization in ARVMs vs. NRVMs (Fig. 4). ARVMs freshly dissociated retain a highly organized sarcomere system and a clear long axis that represents the direction of cell shortening.[31] The perpendicular orientation of ARVMs relative to aligned fibers may reduce resistance to cell shortening.[13] The binding of ARVMs in this orientation is likely driven by the organization of CM integrins, which is tightly coupled to the t-tubule system.[43] On the other hand, freshly isolated NRVMs are round at the time of plating as they lack an organized cytoskeleton.[29] The newly formed cytoskeleton at plating grows in the longitudinal direction of substrate stress, with sarcomeres formed perpendicular to the direction of stress.[20,33]

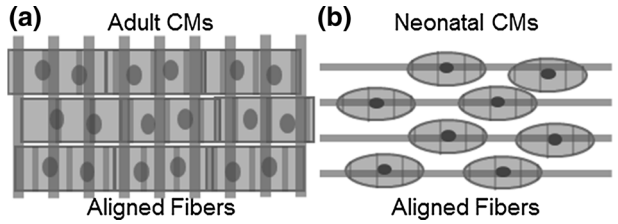

FIGURE 4. Proposed CM cytoskeleton alignment based on cell developmental state. (a) Adult cardiac cells form sarcomeres parallel to aligned ECM fibers and (b) neonatal cardiac cells form sarcomeres perpendicular to aligned ECM fibers.

CONCLUSION

In this study, we demonstrated the importance of ECM microstructure organization in regulating CM phenotype using engineered cardiac-ECM mimetic matrices. SEM images of the human heart revealed fiber alignment as a key feature distinguishing non-failing and failing ventricular myocardial ECM. We were able to adapt electrospinning technology to create substrates that mimicked these alignment properties. The responses of ARVMs to the substrates suggest alignment is a critical component in adult ventricular myocardium that may have importance for CM health. The response of NRVMs to the substrates suggest that there is a marked response (dependent on stage of development) that is critical in determining cell alignment, with a similar response seen in failing adult ventricular myocardium *in vivo*. Our findings suggest, however, that these variations are not to be due to genetic differences in adult myocardium but likely a difference in cytoskeletal organization.

Caution is needed when analyzing data from TCPS cultured CMs, as they are not functionally stable,[1] and progressive changes in CM responses could be a result of subtle alterations to the culture conditions. The

results of this research indicate aligned fiber substrates maintained CM phenotype for an extended period of time, better matching freshly isolated CM morphologically and genetically. More interestingly, culture on such substrates gave insight into different CM organization based on developmental state and ECM organization.

ELECTRONIC SUPPLEMENTARY MATERIAL

The online version of this article (doi:10.1007/s12195-015-0412-9) contains supplementary material, which is available to authorized users.

ACKNOWLEDGMENTS

This study was supported by NIH HL091465, NSF DMR 1006558, U0100398, and AHA 13GRNT 16690019. The authors would also like to acknowledge the use of resources at the Vanderbilt Institute of Nanoscale Science and Engineering (VINSE), a facility renovated under NSF ARI-R2 DMR-0963361.

CONFLICT OF INTEREST

Rutwik Rath, Jung Bok Lee, Truc-Linh Tran, Sean F. Lenihan, Cristi L. Galindo, Yan Ru Su, Tarek Absi, Leon M. Bellan, Douglas B. Sawyer, and Hak-Joon Sung declare that they have no conflicts of interest.

HUMAN AND ANIMAL RIGHTS AND INFORMED CONSENT

All human subject research was carried out in accordance with the guidelines of Vanderbilt IRB and human research protection program and approved by approved by the Vanderbilt Institutional Review Board. All animal studies were carried out in accordance with the guidelines of the Vanderbilt University Animal Care and Use Committee and approved by the Vanderbilt Institutional Review Board.

REFERENCES

[1]Akhyari, P., H. Kamiya, A. Haverich, M. Karck, and A. Lichtenberg. Myocardial tissue engineering: the extracellular matrix. *Eur. J. Cardio-Thorac. Surg.* 34:229–241, 2008.

[2]Ausma, J., and M. Borgers. Dedifferentiation of atrial cardiomyocytes: from in vivo to in vitro. *Cardiovasc. Res.* 55:9–12, 2002.

[3]Bhana, B., R. K. Iyer, W. L. Chen, R. Zhao, K. L. Sider, M. Likhitpanichkul, C. A. Simmons, and M. Radisic. Influence of substrate stiffness on the phenotype of heart cells. *Biotechnol. Bioeng.* 105:1148–1160, 2010.

[4]Bird, S. D., P. A. Doevendans, M. A. van Rooijen, A. de Brutel la Riviere, R. J. Hassink, R. Passier, and C. L. Mummery. The human adult cardiomyocyte phenotype. *Cardiovasc. Res.* 58:423–434, 2003.

[5]Bugaisky, L. B., and R. Zak. Differentiation of adult rat cardiac myocytes in cell culture. *Circ. Res.* 64:493–500, 1989.

[6]Bursac, N., M. Papadaki, R. J. Cohen, F. J. Schoen, S. R. Eisenberg, R. Carrier, G. Vunjak-Novakovic, and L. E. Freed. Cardiac muscle tissue engineering: toward an in vitro model for electrophysiological studies. *Am. J. Physiol.* 277:H433–H444, 1999.

[7]Chlopcikova, S., J. Psotova, and P. Miketova. Neonatal rat cardiomyocytes: a model for the study of morphological, biochemical and electrophysiological characteristics of the heart. *Biomed. Pap. Med. Fac. Univ. Palacký Olomouc Czechoslovakia* 145:49–55, 2001.

[8]Crapo, P. M., T. W. Gilbert, and S. F. Badylak. An overview of tissue and whole organ decellularization processes. *Biomaterials* 32:3233–3243, 2011.

[9]Duling, R. R., R. B. Dupaix, N. Katsube, and J. Lannutti. Mechanical characterization of electrospun polycaprolactone (pcl): a potential scaffold for tissue engineering. *J. Biomech. Eng.* 130:011006–011006, 2008.

[10]Ellingsen, O., A. J. Davidoff, S. K. Prasad, H. J. Berger, J. P. Springhorn, J. D. Marsh, R. A. Kelly, and T. W. Smith. Adult rat ventricular myocytes cultured in defined medium: phenotype and electromechanical function. *Am. J. Physiol.* 265:H747–H754, 1993.

[11]Engelmayr, Jr., G. C., M. Cheng, C. J. Bettinger, J. T. Borenstein, R. Langer, and L. E. Freed. Accordion-like honeycombs for tissue engineering of cardiac anisotropy. *Nat. Mater.* 7:1003–1010, 2008.

[12]Farouz, Y., Y. Chen, A. Terzic, and P. Menasche. Concise review: growing hearts in the right place: on the design of biomimetic materials for cardiac stem cell differentiation. *Stem Cells* 33:1021–1035, 2015.

[13]Galie, P. A., N. Khalid, K. E. Carnahan, M. V. Westfall, and J. P. Stegemann. Substrate stiffness affects sarcomere and costamere structure and electrophysiological function of isolated adult cardiomyocytes. *Cardiovasc. Pathol.* 22:219–227, 2013.

[14]Galindo, C. L., E. Kasasbeh, A. Murphy, S. Ryzhov, S. Lenihan, F. A. Ahmad, P. Williams, A. Nunnally, J. Adcock, Y. Song, F. E. Harrell, T. L. Tran, T. J. Parry, J. Iaci, A. Ganguly, I. Feoktistov, M. K. Stephenson, A. O. Caggiano, D. B. Sawyer, and J. H. Cleator. Anti-remodeling and anti-fibrotic effects of the neuregulin-1beta glial growth factor 2 in a large animal model of heart failure. *J. Am. Heart Assoc.* 3:e000773, 2014.

[15]Golden, H. B., D. Gollapudi, F. Gerilechaogetu, J. Li, R. J. Cristales, X. Peng, and D. E. Dostal. Isolation of cardiac myocytes and fibroblasts from neonatal rat pups. *Methods Mol. Biol.* 843:205–214, 2012.

[16]Gupta, M. K., J. M. Walthall, R. Venkataraman, S. W. Crowder, D. K. Jung, S. S. Yu, T. K. Feaster, X. Wang, T. D. Giorgio, C. C. Hong, F. J. Baudenbacher, A. K. Hatzopoulos, and H.-J. Sung. Combinatorial polymer electrospun matrices promote physiologically-relevant cardiomyogenic stem cell differentiation. *PLoS One* 6:e28935, 2011.

[17]Hang, C. T., J. Yang, P. Han, H. L. Cheng, C. Shang, E. Ashley, B. Zhou, and C. P. Chang. Chromatin regulation by Brg1 underlies heart muscle development and disease. *Nature* 466:62–67, 2010.
[18]Herron, T. J., F. S. Korte, and K. S. McDonald. Loaded shortening and power output in cardiac myocytes are dependent on myosin heavy chain isoform expression. *Am. J. Physiol. Heart Circ. Physiol.* 281(3):H1217–H1222, 2001.
[19]Huang, Y., L. Zheng, X. Gong, X. Jia, W. Song, M. Liu, and Y. Fan. Effect of cyclic strain on cardiomyogenic differentiation of rat bone marrow derived mesenchymal stem cells. *PLoS One* 7:e34960, 2012.
[20]Huyghe, J. M., D. H. van Campen, T. Arts, and R. M. Heethaar. The constitutive behaviour of passive heart muscle tissue: a quasi-linear viscoelastic formulation. *J. Biomech.* 24:841–849, 1991.
[21]Inserte, J., V. Hernando, M. Ruiz-Meana, M. Poncelas-Nozal, C. Fernandez, L. Agullo, C. Sartorio, U. Vilardosa, and D. Garcia-Dorado. Delayed phospholamban phosphorylation in post-conditioned heart favours ca^{2+} normalization and contributes to protection. *Cardiovasc. Res.* 103:542–553, 2014.
[22]Kabaeva, Z., M. Zhao, and D. E. Michele. Blebbistatin extends culture life of adult mouse cardiac myocytes and allows efficient and stable transgene expression. *Am. J. Physiol. Heart Circ. Physiol.* 294:H1667–H1674, 2008.
[23]Kim, D. H., E. A. Lipke, P. Kim, R. Cheong, S. Thompson, M. Delannoy, K. Y. Suh, L. Tung, and A. Levchenko. Nanoscale cues regulate the structure and function of macroscopic cardiac tissue constructs. *Proc. Natl. Acad. Sci. USA* 107:565–570, 2010.
[24]Knöll, R. A role for membrane shape and information processing in cardiac physiology. *Pflug. Arch.* 467:167–173, 2015.
[25]Kovács, M., J. Tóth, C. Hetényi, A. Málnási-Csizmadia, and J. R. Sellers. Mechanism of blebbistatin inhibition of myosin II. *J. Biol. Chem.* 279:35557–35563, 2004.
[26]Kubin, T., J. Pöling, S. Kostin, P. Gajawada, S. Hein, W. Rees, A. Wietelmann, M. Tanaka, H. Lörchner, S. Schimanski, M. Szibor, H. Warnecke, and T. Braun. Oncostatin m is a major mediator of cardiomyocyte dedifferentiation and remodeling. *Cell Stem Cell* 9:420–432, 2011.
[27]Kuo, P.-L., H. Lee, M.-A. Bray, N. A. Geisse, Y.-T. Huang, W. J. Adams, S. P. Sheehy, and K. K. Parker. Myocyte shape regulates lateral registry of sarcomeres and contractility. *Am. J. Pathol.* 181:2030–2037, 2012.
[28]Lakshmanan, R., U. M. Krishnan, and S. Sethuraman. Living cardiac patch: the elixir for cardiac regeneration. *Expert Opin. Biol. Ther.* 12:1623–1640, 2012.
[29]Louch, W. E., K. A. Sheehan, and B. M. Wolska. Methods in cardiomyocyte isolation, culture, and gene transfer. *J. Mol. Cell. Cardiol.* 51:288–298, 2011.
[30]Lutolf, M. P., and J. A. Hubbell. Synthetic biomaterials as instructive extracellular microenvironments for morphogenesis in tissue engineering. *Nat. Biotechnol.* 23:47–55, 2005.
[31]McCain, M. L., and K. K. Parker. Mechanotransduction: the role of mechanical stress, myocyte shape, and cytoskeletal architecture on cardiac function. *Pflug. Arch.* 462:89–104, 2011.
[32]Mitcheson, J. S., J. C. Hancox, and A. J. Levi. Action potentials, ion channel currents and transverse tubule density in adult rabbit ventricular myocytes maintained for 6 days in cell culture. *Pflug. Arch.* 431:814–827, 1996.
[33]Modis, L. Organization of the extracellular matrix. Taylor & Francis: CRC Press, 1990.
[34]Morrisey, E. E. Rewind to recover: dedifferentiation after cardiac injury. *Cell Stem Cell* 9:387–388, 2011.
[35]Norris, R. A., T. K. Borg, J. T. Butcher, T. A. Baudino, I. Banerjee, and R. R. Markwald. Neonatal and adult cardiovascular pathophysiological remodeling and repair. *Ann. N. Y. Acad. Sci.* 1123:30–40, 2008.
[36]Parameswaran, S., S. Kumar, R. S. Verma, and R. K. Sharma. Cardiomyocyte culture: an update on the in vitro cardiovascular model and future challenges. *Can. J. Physiol. Pharmacol.* 91:985–998, 2013.
[37]Patel, A., B. Fine, M. Sandig, and K. Mequanint. Elastin biosynthesis: the missing link in tissue-engineered blood vessels. *Cardiovasc. Res.* 71:40–49, 2006.
[38]Sander, V., G. Suñe, C. Jopling, C. Morera, and J. C. I. Belmonte. Isolation and in vitro culture of primary cardiomyocytes from adult zebrafish hearts. *Nat. Protoc.* 8:800–809, 2013.
[39]Shutova, M., C. Yang, J. M. Vasiliev, and T. Svitkina. Functions of nonmuscle myosin II in assembly of the cellular contractile system. *PLoS One* 7:e40814, 2012.
[40]Simpson, D. G., L. Terracio, M. Terracio, R. L. Price, D. C. Turner, and T. K. Borg. Modulation of cardiac myocyte phenotype in vitro by the composition and orientation of the extracellular matrix. *J. Cell. Physiol.* 161:89–105, 1994.
[41]Sreejit, P., and R. S. Verma. Natural ECM as biomaterial for scaffold based cardiac regeneration using adult bone marrow derived stem cells. *Stem Cell Rev.* 9:158–171, 2013.
[42]Stout, D. A., J. Yoo, A. N. Santiago-Miranda, and T. J. Webster. Mechanisms of greater cardiomyocyte functions on conductive nanoengineered composites for cardiovascular application. *Int. J. Nanomed.* 7:5653–5669, 2012.
[43]Valencik, M. L., D. Zhang, B. Punske, P. Hu, J. A. McDonald, and S. E. Litwin. Integrin activation in the heart: a link between electrical and contractile dysfunction? *Circ. Res.* 99:1403–1410, 2006.
[44]Wang, N., K. Burugapalli, W. Song, J. Halls, F. Moussy, Y. Zheng, Y. Ma, Z. Wu, and K. Li. Tailored fibro-porous structure of electrospun polyurethane membranes, their size-dependent properties and trans-membrane glucose diffusion. *J. Membr. Sci.* 427:207–217, 2013.
[45]Wendel, J. S., L. Ye, P. Zhang, R. T. Tranquillo, and J. J. Zhang. Functional consequences of a tissue-engineered myocardial patch for cardiac repair in a rat infarct model. *Tissue Eng. Part A.* 20:1325–1335, 2014.